INL REPORT

INL/EXT-15-36771
Unlimited Release
September 2015

RELAP-7 Progress Report: FY-2015 Optimization Activities Summary

Prepared by
Idaho National Laboratory
Idaho Falls, Idaho 83415

The Idaho National Laboratory is a multiprogram laboratory operated by
Battelle Energy Alliance for the United States Department of Energy
under DOE Idaho Operations Office. Contract DE-AC07-05ID14517.

Issued by the Idaho National Laboratory, operated for the United States Department of Energy by Battelle Energy Alliance.

Printed in the United States of America. This report has been reproduced directly from the best available copy.

INL/EXT-15-36771
Unlimited Release
September 2015

RELAP-7 Progress Report: FY-2015 Optimization Activities Summary

R. A. Berry, L. Zou, D. Andrs, R. C. Martineau

Contents

Summary 8
1 Introduction 9
2 Brief Review of Nonequilibrium, 2-Pressure, 7-Equation Two-Phase Model 10
3 Spline-Based Table Look-up (SBTL) Method for Steam and Water Properties . . 14
3.1 Property Functions Given by the Modified SBTL Package 16
4 Stabilizing Entropy Viscosity Method 19
5 Implementation of Two-phase Flow Closure Correlations 23
References 31

Figures

1 $(\bar{v}, e)$ state space spline polynomial cell, with node (center circle), knots (corner squares), and mid-points (edge x's) plus neighboring cells and nodes. 17
2 Flow regimes in vertical pipes used in TRACE code 24
3 Flow regimes in horizontal pipes used in TRACE code 28
4 Post-CHF flow regimes in vertical pipes used in TRACE code 30

Tables

1 Closure correlations related to pre-CHF flow regimes in vertical pipes 28
2 Closure correlations related to pre-CHF flow regimes in horizontal pipes . . 29
3 Closure correlations related to post-CHF flow regimes in vertical pipes 29

Summary

This report summarily documents the optimization activities on RELAP-7 for FY-2015. It includes the migration from the analytical stiffened gas equation of state (for both the vapor and liquid phases) to accurate and efficient property evaluations for both equilibrium and metastable (nonequilibrium) states, using the Spline-Based Table Look-up (SBTL) method with the IAPWS-95 properties for steam and water. It also includes the initiation of realistic closure models based, where appropriate, on the U.S. Nuclear Regulatory Commission's TRACE code. It also describes an improved entropy viscosity numerical stabilization method for the nonequilibrium two-phase flow model of RELAP-7. For ease of presentation to the reader, the nonequilibrium two-phase flow model used in RELAP-7 is briefly presented, though for detailed explanation the reader is referred to *RELAP-7 Theory Manual* [R.A. Berry, J.W. Peterson, H. Zhang, R.C. Martineau, H. Zhao, L. Zou, D. Andrs, "RELAP-7 Theory Manual," *Idaho National Laboratory INL/EXT-14-31366 (rev. 1)*, February 2014].

1 Introduction

This report documents the optimization activities on RELAP-7 for FY-2015. It includes the migration from the analytical stiffened gas equation of state for both the vapor and the liquid phases to accurate and efficient property calculations for each. It also includes an initiation of realistic closures models, as well as an improved entropy viscosity stabilization method. For ease of presentation, the nonequilibium two-phase model used by RELAP-7 is briefly summarized. The equations are given without detailed explanation and the reader is referred to [1] for details.

2 Brief Review of Nonequilibrium, 2-Pressure, 7-Equation Two-Phase Model

The RELAP-7 light water nuclear reactor system analysis code allows the use of two different two-phase models: (1) a *homogeneous equilibrium model (HEM)* which has three governing balance equations, and (2) the fully nonequilibrium, 2-pressure model which has seven governing balance equations. The balance equations (volume fraction evolution, mass, momentum, and total energy for each phase) for the *nonequilibrium 7-equation model (SEM)* [1] are recalled:

$$\begin{aligned}\frac{\partial \alpha_{liq} A}{\partial t} + u_{int} A \frac{\partial \alpha_{liq}}{\partial x} &= A\mu(p_{liq} - p_{vap}) - \frac{\Gamma_{int,vap} A_{int} A}{\rho_{int}} - \frac{\Gamma_{wall,vap}}{\rho_{int}} \\ &+ \frac{\partial \mathcal{U}_{liq}}{\partial x}\end{aligned} \tag{1}$$

$$\frac{\partial \left(\alpha\rho\right)_{liq} A}{\partial t} + \frac{\partial \left(\alpha\rho u\right)_{liq} A}{\partial x} = -\Gamma_{int,vap} A_{int} A - \Gamma_{wall,vap} + \frac{\partial \mathcal{F}_{liq}}{\partial x} \tag{2}$$

$$\begin{aligned}\frac{\partial \left(\alpha\rho u\right)_{liq} A}{\partial t} + \frac{\partial \alpha_{liq} A \left(\rho u^2 + p\right)_{liq}}{\partial x} &= p_{int} A \frac{\partial \alpha_{liq}}{\partial x} + p_{liq} \alpha_{liq} \frac{\partial A}{\partial x} \\ &+ A\lambda(u_{vap} - u_{liq}) \\ &- \Gamma_{int,vap} A_{int} u_{int} A - \Gamma_{wall,vap} u_{int} \\ &- F_{\text{wall friction},liq} - F_{\text{friction},vap} \\ &+ \left(\alpha\rho\right)_{liq} A \boldsymbol{g} \cdot \hat{n}_{axis} \\ &+ \frac{\partial \mathcal{G}_{liq}}{\partial x}\end{aligned} \tag{3}$$

$$\begin{aligned}\frac{\partial\left(\alpha\rho E\right)_{liq}A}{\partial t}+\frac{\partial\alpha_{liq}u_{liq}A\left(\rho E+p\right)_{liq}}{\partial x}&=p_{int}u_{int}A\frac{\partial\alpha_{liq}}{\partial x}-\bar{p}_{int}A\mu(p_{liq}-p_{vap})\\&+\bar{u}_{int}A\lambda(u_{vap}-u_{liq})\\&+\Gamma_{int,vap}A_{int}\left(\frac{p_{int}}{\rho_{int}}-H_{liq,int}\right)A\\&+A_{int}h_{conv,liq}(T_{int}-T_{liq})A\\&+h_{wall,liq,conv}(T_{wall}-T_{liq})\,\kappa\,P_{hf}\\&-\Gamma_{wall,vap}\left(-\frac{p_{int}}{\rho_{int}}+h_{vap,int}+\frac{u_{int}^2}{2}\right)\\&+\left(\alpha\rho u\right)_{liq}A\boldsymbol{g}\cdot\hat{n}_{axis}\\&+\frac{\partial\left(\mathfrak{h}_{liq}+u_{liq}\mathfrak{g}_{liq}\right)}{\partial x}\end{aligned}\tag{4}$$

for the liquid phase, and

$$\begin{aligned}\frac{\partial\alpha_{vap}A}{\partial t}+u_{int}A\frac{\partial\alpha_{vap}}{\partial x}&=A\mu(p_{vap}-p_{liq})+\frac{\Gamma_{int,vap}A_{int}A}{\rho_{int}}+\frac{\Gamma_{wall,vap}}{\rho_{int}}\\&+\frac{\partial\mathfrak{l}_{vap}}{\partial x}\end{aligned}\tag{5}$$

$$\frac{\partial\left(\alpha\rho\right)_{vap}A}{\partial t}+\frac{\partial\left(\alpha\rho u\right)_{vap}A}{\partial x}=\Gamma_{int,vap}A_{int}A+\Gamma_{wall,vap}+\frac{\partial\mathfrak{f}_{vap}}{\partial x}\tag{6}$$

$$\begin{aligned}\frac{\partial\left(\alpha\rho u\right)_{vap}A}{\partial t}+\frac{\partial\alpha_{vap}A\left(\rho u^2+p\right)_{vap}}{\partial x}&=p_{int}A\frac{\partial\alpha_{vap}}{\partial x}+p_{vap}\alpha_{vap}\frac{\partial A}{\partial x}\\&+A\lambda(u_{liq}-u_{vap})\\&+\Gamma_{int,vap}A_{int}u_{int}A+\Gamma_{wall,vap}u_{int}\\&-F_{\text{wall friction},vap}-F_{\text{friction},liq}\\&+\left(\alpha\rho\right)_{vap}A\boldsymbol{g}\cdot\hat{n}_{axis}\\&+\frac{\partial\mathfrak{g}_{vap}}{\partial x}\end{aligned}\tag{7}$$

$$\frac{\partial\left(\alpha\rho E\right)_{vap}A}{\partial t}+\frac{\partial\alpha_{vap}u_{vap}A\left(\rho E+p\right)_{vap}}{\partial x}=p_{int}u_{int}A\frac{\partial\alpha_{vap}}{\partial x}-\bar{p}_{int}A\mu(p_{vap}-p_{liq})$$
$$+\bar{u}_{int}A\lambda(u_{liq}-u_{vap})$$
$$-\Gamma_{int,vap}A_{int}\left(\frac{p_{int}}{\rho_{int}}-H_{vap,int}\right)A$$
$$+A_{int}h_{conv,vap}(T_{int}-T_{vap})A$$
$$+h_{wall,vap,conv}(T_{wall}-T_{vap})(1-\kappa)P_{hf}$$
$$+\Gamma_{wall,vap}\left(-\frac{p_{int}}{\rho_{int}}+h_{vap,int}+\frac{u_{int}^{2}}{2}\right)$$
$$+\left(\alpha\rho u\right)_{vap}A\boldsymbol{g}\cdot\hat{n}_{axis}$$
$$+\frac{\partial\left(\mathfrak{h}_{vap}+u_{vap}\mathfrak{g}_{vap}\right)}{\partial x} \tag{8}$$

for the vapor phase. The eighth equation can be eliminated for two phases by recognizing that $\alpha_{vap}=1-\alpha_{liq}$. The terms shown in red are viscous regularization terms added to the *SEM* to help assure uniqueness of the weak hyperbolic solutions, and primarily to provide numerical stabilization with the entropy viscosity method, which will be discussed below. The nomenclature is somewhat standard and again the reader is referred to [1] for details.

The interface average pressure and average velocity are given by:

$$p_{int}=\frac{z_{liq}p_{vap}+z_{vap}p_{liq}}{z_{liq}+z_{vap}} \tag{9}$$

$$u_{int}=\frac{z_{liq}u_{liq}+z_{vap}u_{vap}}{z_{liq}+z_{vap}} \tag{10}$$

where $z_k=\rho_k w_k$, $(k=liq,\,vap)$ are the phasic acoustic impedances with w_k being the phasic sound speeds. The interface saturation temperature is determined from the calculated interface pressure $T_{int}=T_{sat}(p_{int})$, the phasic enthalpies $h_{liq,sat}$ and $h_{vap,sat}$ are determined at this saturation temperature T_{sat}, and the heat of vaporization $\delta h_{vap}(T_{sat})=h_{vap,sat}(T_{sat})-h_{liq,sat}(T_{sat})$ is also determined.

Total saturated phasic enthalpies are given by:

$$H_{liq,sat} = h_{liq,sat} + 0.5u_{int}^2 \tag{11}$$
$$H_{vap,sat} = h_{vap,sat} + 0.5u_{int}^2 \tag{12}$$

and the total heat of vaporization at $T_{int} = T_{sat}$ by

$$\delta h_{tot}(T_{sat}) = H_{vap,sat} - H_{liq,sat}. \tag{13}$$

This step, however, is not necessary because in this case $\delta h_{tot}(T_{sat})$ and $\delta h_{vap}(T_{sat})$ are identical.

The interphase mass transfer rate (per unit interfacial area) per unit volume coming from the liquid phase across the interfacial area is computed by:

$$\Gamma_{int,vap} = \frac{h_{conv,liq}(T_{liq} - T_{int}) + h_{conv,vap}(T_{vap} - T_{int})}{\delta h_{vap}(T_{sat})}\,. \tag{14}$$

Note, additional vapor will be generated at the wall, $\Gamma_{wall,vap}$, due to local wall boiling such that $\Gamma_{vap}A = \Gamma_{int,vap}A_{int}A + \Gamma_{wall,vap}$. The simple wall boiling model is also described in [1].

3 Spline-Based Table Look-up (SBTL) Method for Steam and Water Properties

For the simulation of two-phase flows with RELAP-7 accurate equations of state must be used to obtain the properties of steam and water. Moreover, for CPU-intensive numerical simulations with this code thermodynamic and transport properties of steam and water are calculated extremely often. Because the dependent variable of the two-phase model partial differential equations are mass-, momentum-, and total energy-densities the thermodynamically independent variables of the required property functions are specific volume and specific internal energy (v, e). These are readily computed from the phasic dependent variables as

$$v_k = \frac{1}{\rho_k} = \frac{\alpha_k}{(\alpha\rho)_k}, \qquad k = \{liq, vap\} \tag{15}$$

$$e_k = \frac{(\alpha\rho E)_k}{(\alpha\rho)_k} - \frac{1}{2}\frac{(\alpha\rho u)_k^2}{(\alpha\rho)_k^2}, \qquad k = \{liq, vap\}\ . \tag{16}$$

Then other phasic properties are functions of these two phasic thermodynamic properties, e.g. pressure $p_k = f\left(v_k, e_k\right)$.

Determining properties as a function of (v, e) from an accurate equation of state such as IAPWS-95 would normally require backward functions for calculations from pressure and specific volume (p, v) and specific internal energy and specific entropy (e, s). This requires an iterative solution that is very time-consuming and not computationally efficient. Therefore, in the original development of RELAP-7 property calculations were simplified through the use of the stiffened gas equation of state for each phase [1]. These simplifications cause, depending on the range of state, inaccuracies in the results of the reactor system simulation. To provide fast and accurate property calculation algorithms, RELAP-7 was modified to employ the Spline-Based Table Look-up (SBTL) Method [2] which was developed in a project of the International Association for the Properties of Water and Steam (IAPWS). With this method properties from existing accurate equations of state, such as IAPWS-95 for steam and water, can be reproduced with high accuracy and significantly reduced computational times. Under INL direction, the SBTL method based on the IAPWS-95 properties for steam and water was extensively modified for RELAP-7,

by Matthias Kunick at Zittau/Goerlitz University of Applied Sciences [3], to allow the calculation of not just the equilibrium properties for the homogeneous equilibrium model (HEM), but also to provide the metastable properties that are needed by the 7-equation, nonequilibrium, two-pressure model.

Table look-up methods can be well-suited for fast and accurate property calculations. A table is populated with discrete values of the required properties which are calculated from an available equation of state such as IAPWS-95. During the simulation process, properties are determined from this look-up table through the use of simple interpolation and approximation algorithms. The Spline-Based Table Look-up (SBTL) method [2] applies polynomial spline interpolation techniques to reproduce the results of the IAPWS-95 equation of state with high accuracy and low computing time. It employs specialized coordinate transformations and simplified search algorithms to minimize the computing time and to optimize the look-up table for the desired accuracy [4].

For the numerical process simulations here, the continuous, piecewise defined spline functions need additionally to be only once continuously differentiable. Therefore the SBTL method utilizes a simple bi-quadratic spline polynomial which offers the additional advantage of being analytically solvable in terms of the independent variables. This latter property allows the calculation of the inverse spline functions, i.e. the numerically consistent backward functions. Because the bi-quadratic polynomial spline has a constant second derivative which precludes its capture of changing curvature, SBTL method allows the transformation of the variables of the interpolated function in order to minimize the third derivative, i.e. the coordinates are transformed in such manner that the change in curvature of the underlying function is reduced. This allows the spline polynomial to reproduce the transformed property function more easily and with greater accuracy [4]. For the version of SBTL utilized for RELAP-7, the specific internal energy *e* is not transformed while the specific volume is transformed as $\bar{v} = ln(v)$.

For example, a two-dimensional spline-based property function, such as pressure, for the liquid phase would be written $p^L(\bar{v}, e)$ while the same property for the vapor (gas) phase would be written $p^G(\bar{v}, e)$. In the RELAP-7 nonequilibrium, 7-equation two-phase model the phasic specific internal energies and phasic transformed specific volumes are passed, respectively, to compute each corresponding phasic property function. It is important to point out that for the 7-equation two-phase model, these phasic property functions can be either normal (equilibrium) single phase values or metastable (nonequilibrium) single phase values.

For the SBTL Method the spline function is created in transformed coordinates and interpolates values between a logically rectangular set of discrete data points called *nodes*. The locally defined spline polynomials are defined over a local rectangular cell having a *node* at its center and *knots* at its four corners. Four polynomial cells are connected at each *knot*, see Figure 1. The equidistant nodes (in transformed space) are distributed in a manner to insure the required accuracy of the spline function over the full range of validity. An efficient search algorithm is employed to rapidly determine the grid cell in which an arbitrary $(\bar{v}, e)$ is located. The locally defined polynomial must intersect the cell node, e.g. $p^L_{i,j}(\bar{v}_i, e_j)$, while its partial state derivatives with respect to $\bar{v}$ and e must match at the right and left edges midway between the nodes in the horizontal direction and, respectively, the top and bottom edges midway between nodes in the vertical direction. At the cell corners, *knots*, the cross derivatives of all four contiguous cells must match. The equations representing these conditions, the composite of all of these nine-point stencil cells, form a system of equations that are solved globally to yield the local polynomial coefficients for each cell [2] [5]. Technical details of the SBTL method as developed for the two-phase models of RELAP-7 will be documented at a later date in an updated version of the RELAP-7 Theory Manual [1].

The SBTL method was applied to industrial formulation IAPWS-IF97 in [4] and tested in multidimensional CFD simulations of condensing steam in a turbine cascade. With this approach to obtaining real fluid properties the computing times were increased by a factor of only 1.4 over the same calculation using analytical ideal gas values, and these CFD simulations using the SBTL method were 6-10 times faster than using IAPWS-IF97 directly [4] (presumably in an iterative manner).

3.1 Property Functions Given by the Modified SBTL Package

The following thermodynamic and transport properties are provided by the modified SBTL Package for equiliibrium mixture and for each phase (stable and metastable) as a function of respective phasic specific volume v and specific energy e, as well partial derivatives of the property with respect to v and e (it is recalled that RELAP-7 [1] employs implicit temporal integration and needs a Jacobian which is based on these derivatives):

$p(v, e)$ – pressure
$T(v, e)$ – temperature
$w(v, e)$ – sound speed
$c_p(v, e)$ – isobaric specific heat

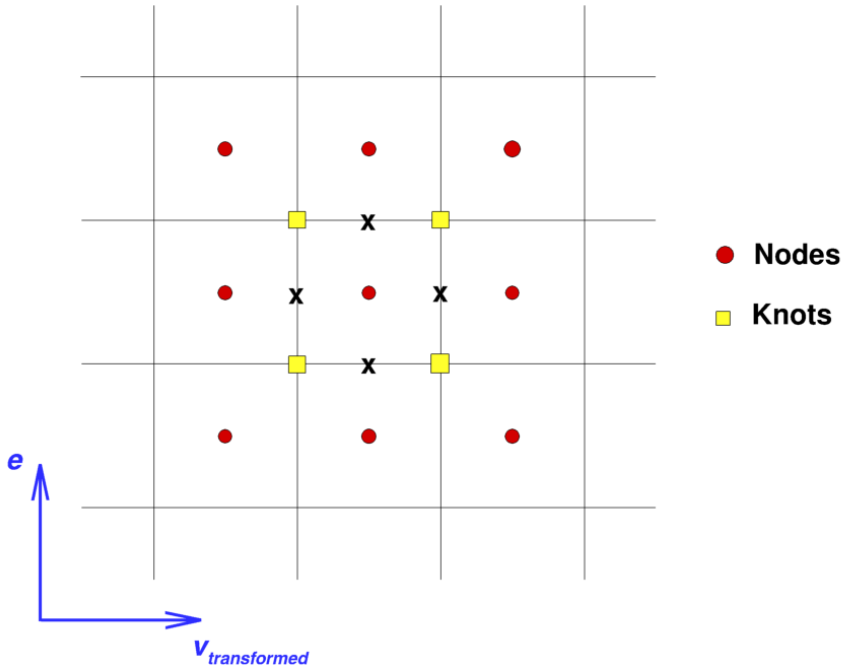

Figure 1. $(\bar{v}, e)$ state space spline polynomial cell, with node (center circle), knots (corner squares), and mid-points (edge x's) plus neighboring cells and nodes.

$c_v(v, e)$ – isochoric specific heat
$g(v, e)$ – Gibbs energy
$s(v, e)$ – specific entropy

$k(v, e)$ – thermal conductivity
$\nu(v, e)$ – dynamic viscosity
$\sigma(T(v, e))$ – surface tension.

For convenience the following functions of, and partial derivatives with respect to, pressure p and temperature T are also provided:

$\rho(p, T)$ – mass density ($1/v$) as a function of pressure and temperature
$e(p, T)$ – specific internal energy as a function of pressure and temperature.

Lastly, the following functions of, and partial derivatives with respect to, pressure p and temperature T at saturation are provided:

$T_{sat}(p)$ – saturation temperature as a function of pressure
$p_{sat}(T)$ – saturation pressure as function of temperature
δh_{vap} – heat of vaporization.

4 Stabilizing Entropy Viscosity Method

Under INL direction, the viscous regularization for the 7-equation two-phase model of RELAP-7 given above was obtained, by Marco Delchini at Texas A&M University, using the similar methodology to that for the Euler equations [6]. The method consists of adding dissipative terms to the system of governing balance equations and in deriving an entropy equation for the regularized system. By adequately selecting these artificial viscous fluxes, the sign of the entropy production remains positive, ensuring uniqueness of the numerical solution. Derivation of the viscous regularization for the *SEM* can be achieved by considering either the phasic entropy equation or the total entropy equation. In the latter case, the minimum entropy principle can be established for the whole two-phase system but may not ensure positivity of the entropy equation for each phase. However, positivity of the total entropy equation can also be achieved by requiring that the minimum entropy principle holds for each phase. This stronger requirement has the advantage of ensuring consistency with the single-phase Euler equations when one of the phases disappears in the limit of phase disappearance.

In the red terms of the balance equations above for the nonequilibrium two-phase *SEM*, $\mathfrak{f}_k, \mathfrak{g}_k, \mathfrak{h}_k$, and $\mathfrak{l}_k$, with $k = \{liq,\ vap\}$, are phasic viscous terms to be specified. The *SEM* without the viscous regularization terms is, by design, entropy producing. The *SEM* with the regularization terms must also be entropy producing. To verify the entropy production of the *SEM* with regularization terms we therefore need only consider the regularization terms. The phasic entropy equation with only the regularization terms is

$$\alpha_k \rho_k A \frac{Ds_k}{Dt} = \left[(\rho s_\rho)_k - (e s_e)_k\right] \frac{\partial \mathfrak{f}_k}{\partial x} - \rho_k^2 (s_\rho)_k \frac{\partial \mathfrak{l}_k}{\partial x} + (s_e)_k \frac{\partial \left(\mathfrak{h}_k + \frac{1}{2} u_k^2 \mathfrak{f}_k\right)}{\partial x} + (s_e)_k \left(\mathfrak{g}_k - \mathfrak{f}_k u_k\right) \frac{\partial u_k}{\partial x}. \quad (17)$$

Because the right hand side of this equation must be greater than zero, by the minimum entropy principle, at a point where the entropy $s_k(\rho_k, e_k)$ reaches its minimum value, the gradient $\nabla_{\rho_k, e_k}(s_k)$ must be zero and the Laplacian $\triangle_{\rho_k, e_k}(s_k)$ must be positive; see e.g. [7]. It can be shown [8] that a way to ensure this principle is to require

$$\mathfrak{l}_k = \beta_k A \frac{\partial \alpha_k}{\partial x} \tag{18}$$

$$\mathfrak{f}_k = \alpha_k \kappa_k A \frac{\partial \rho_k}{\partial x} + \rho_k \mathfrak{l}_k \tag{19}$$

$$\mathfrak{g}_k = \alpha_k \mu_k \rho_k A \frac{\partial u_k}{\partial x} + \mathfrak{f}_k u_k \tag{20}$$

$$\mathfrak{h}_k = \alpha_k \kappa_k A \frac{\partial \left(\rho e\right)_k}{\partial x} - \frac{u_k^2}{2} \mathfrak{f}_k + \left(\rho e\right)_k \mathfrak{l}_k \tag{21}$$

where β_k, μ_k, and κ_k are positive coefficients to be specified (note: the phasic, subscripted parameter κ_k here is not to be confused with the unsubscripted κ appearing in the total energy balance equations).

Because two-phase flows may be found in a wide range of speeds, from extremely low-Mach subsonic (nearly incompressible) to supersonic, these three positive viscous coefficients are designed, from the scaled *SEM*, to ensure well-scaled dissipative terms over the entire range of Mach numbers of interest. When artificial viscosity techniques are used, sufficient artificial viscosity must be present in the shock and discontinuity regions to prevent spurious oscillations from forming in the numerical solution, but little or no dissipation should be present where the solution is smooth. It is also imperative that viscosity coefficients scale properly to ensure recovery (locally and dynamically) of the incompressible equations in the low-Mach asymptotic limit. Careful analysis has resulted in the following definitions for the viscous regularization coefficients:

$$\beta_k \left(x,t\right) = min\left(\beta_{k,e}\left(x,t\right), \beta_{k,max}\left(x,t\right)\right) \tag{22}$$
$$\mu_k \left(x,t\right) = min\left(\mu_{k,e}\left(x,t\right), \mu_{k,max}\left(x,t\right)\right) \tag{23}$$
$$\kappa_k \left(x,t\right) = min\left(\kappa_{k,e}\left(x,t\right), \kappa_{k,max}\left(x,t\right)\right) \tag{24}$$

where the definitions of the entropy viscosity coefficients with subscript e and the first-order viscosity coefficents (ceiling values) with subscript max are given, respectively, by

$$\beta_{k,e}\left(x,t\right)=h^{2}\frac{max\left(\left|R_{k}^{\alpha}\left(x,t\right)\right|,J_{k}^{\alpha}\right)}{\left|s_{k}-\bar{s}_{k}\right|_{\infty}} \tag{25}$$

$$\mu_{k,e}\left(x,t\right)=h^{2}\frac{max\left(\left|\tilde{R}_{k}\left(x,t\right)\right|,J_{k}\right)}{\left(1-\sigma\left(M_{k}\right)\right)\rho_{k}w_{k}^{2}+\sigma\left(M_{k}\right)\rho_{k}u_{k}^{2}} \tag{26}$$

$$\kappa_{k,e}\left(x,t\right)=h^{2}\frac{max\left(\left|\tilde{R}_{k}\left(x,t\right)\right|,J_{k}\right)}{\rho_{k}w_{k}^{2}} \tag{27}$$

$$\beta_{k,max}\left(x,t\right)=\mu_{k,max}\left(x,t\right)=\kappa_{k,max}\left(x,t\right)=\frac{h}{2}\left(\left|u_{k}\right|+w_{k}\right)\ . \tag{28}$$

In the above

$$\tilde{R}_{k}\left(x,t\right)=\frac{Dp_{k}\left(x,t\right)}{Dt}-w_{k}^{2}\left(x,t\right)\frac{D\rho_{k}\left(x,t\right)}{Dt} \tag{29}$$

$$R_{k}^{\alpha}\left(x,t\right)=\frac{\partial\left(As_{k}\right)}{\partial t}+Au_{int}\frac{\partial s_{k}}{\partial x} \tag{30}$$

$$J_{k}=\left|u_{k}\right|\ max\left(J\left[p_{k}\right],w_{k}^{2}J\left[\rho_{k}\right]\right) \tag{31}$$

$$J_{k}^{\alpha}=\left|u_{int}\right|\ J\left[\alpha_{k}\right] \tag{32}$$

with $\bar{s}_k$ denoting the average of s_k over the computational domain, $J\left[\cdot\right]$ denoting the jump in function $(\cdot)$, and h representing the element characteristic size (for example, when considering a cell of volume V belonging to a mesh of dimension r then $h=V^{\frac{1}{r}}$). In the denominator of the equation for $\mu_{k,e}$ above, the parametric function $\sigma\left(M_k\right)$ is a weighting

function designed to change the normalization for low-Mach number flows; this parameter is important for the success of the entropy viscosity method for all-speed flows.

This definition of the phasic viscosity coefficients takes advantage of the properties of the entropy residual that is peaked in the vicinity of the shock, whereby the high-order viscosity coefficient will saturate to the first-order viscosity coefficient that is known to be over-dissipative. Moreover, in regions where the numerical solution is smooth, the phasic viscosity coefficient will be equal to the high-order viscosity coefficient that will ensure higher order accuracy and also the correct low-Mach asymptotic limit.

5 Implementation of Two-phase Flow Closure Correlations

During FY-2015, besides the implementation of SBTL for steam and water properties and extension of the entropy viscosity method for the *SEM*, efforts were also begun to implement realistic two-phase closure correlations into the RELAP-7 code. Due to the large quantity of two-phase flow closure correlations required in a system analysis code, their implementation is expected to be a multiple-year effort. This section provides an overview of the initial implementation of these closure correlations, its current status, and future plans.

The two-phase nonequilibrium *SEM*, by itself, is not a closed system without the addition of two-phase flow closure relations which correlate sub-cellular behaviors with experimental data. Such behaviors include both complex mechanical- and thermal-interactions between the two phases as well as interactions of the phases with the wall. Several simplified closure correlations have been implemented in the beta release of the RELAP-7 code [9]. However, successful application using the *SEM* to accurately model a nuclear reactor system requires accurate closures to be implemented with the mass, momentum, and energy conservation equations. During the development of existing system analysis codes, such as TRACE [10], similar closure correlations were developed by other researchers to describe the complex interface and wall-to-fluids behaviors of two-phase flow. In general, these closure correlations include models to define two-phase flow regimes, models to define flow regime dependent interfacial friction, heat and mass transfers, models to define heat transfer between fluids and wall, models for wall friction, models to predict interfacial area density, etc., and are similar to those needed for RELAP-7. Therefore, where appropriate, our initial detailed correlations will, for developmental economy, borrow from TRACE.

In FY-2015, work was initiated to implement closure correlations for wall friction (drag), interfacial friction (drag), interfacial heat transfer, and wall heat transfer in vertical pipes, which correspond to $F_{\text{wall friction},liq}$ and $F_{\text{wall friction},vap}$, $F_{\text{friction},liq}$ and $F_{\text{friction},vap}$, $h_{conv,liq}$ and $h_{conv,vap}$, and $h_{wall,liq,conv}$ and $h_{wall,vap,conv}$, respectively, in the 7-equation model. Many of these correlations are flow regime dependent, i.e. they depend upon the topology or spatial distribution of the phases. Implementation of a flow regime map in vertical pipes has been included in the work in FY-2015. Models have been implemented to determine the local flow regime based on local thermal-hydraulics and geometry conditions, such as pipe diameter, liquid and vapor mass fluxes, void fraction, etc. In addition, proper flow regime dependent correlations are, or will be, chosen based on local flow regime informa-

tion, e.g., using a specific single correlation, proper linear or power-law average of several correlations. Figure 2 shows typical pre-CHF (Critical Heat Flux) flow regimes in vertical pipes used in the TRACE code [10]. Following the same simplification made in TRACE, slug and Taylor cap bubble flow regimes are combined in RELAP-7 into a single flow regime, cap/slug flow regime.

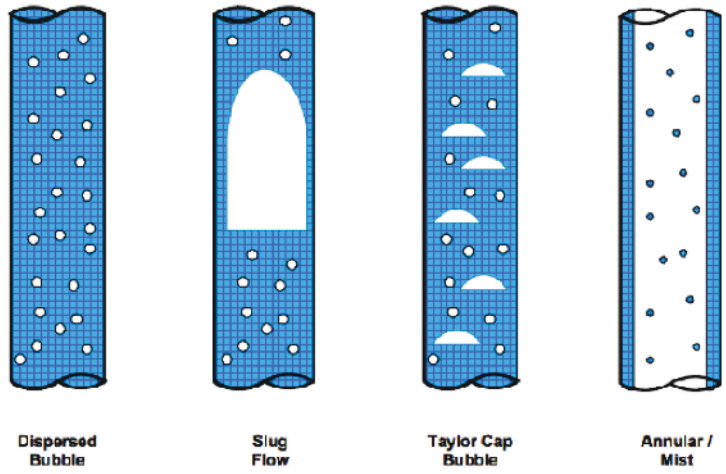

Figure 2. Flow regimes in vertical pipes used in TRACE code [10]

Examples are given in this section for the implementations of aforementioned closure correlations. In TRACE, volumetric interfacial friction, i.e. friction force acting between the two phases, is calculated using relative velocity between two phases and interfacial friction coefficient,

$$f_{int} = C_i u_r \left| u_r \right| \tag{33}$$

in which, C_i is the interfacial friction coefficient, and $u_r = u_{vap} - u_{liq}$ is the relative velocity between the two phases. Drift flux based models are used to calculate C_i,

$$C_i = \frac{\alpha(1-\alpha)^3 g \Delta\rho}{\bar{v}_{gj}^2} P_s \tag{34}$$

in which, $\alpha = \alpha_{vap}$ is volume fraction of the vapor phase, normally referred as void fraction. g is the gravitational constant. Here $\Delta\rho$ is the density difference between the two phases. $\bar{v}_{gj}$ is the weighted mean drift flux velocity. P_s is the profile slip factor, which is calculated as,

$$P_s = \frac{\left(\frac{1-C_0\alpha}{1-\alpha} u_{vap} - C_0 u_{liq}\right)^2}{u_r^2} \tag{35}$$

in which, C_0 is distribution parameter. Both $\bar{v}_{gj}$ and C_0 are drift flux model related parameters, which are flow regime dependent. For bubbly flow regime, they are calculated as,

$$\bar{v}_{gj} = \sqrt{2}\left(\frac{\sigma g \Delta\rho}{\rho_l^2}\right)^{1/4} \tag{36}$$

and

$$C_0 = 1.2 - 0.2\sqrt{\frac{\rho_{vap}}{\rho_{liq}}}\,. \tag{37}$$

Similar correlations have been implemented in the RELAP-7 code to predict interfacial friction.

In the *SEM* the wall friction terms, $F_{\text{wall friction},liq}$ and $F_{\text{wall friction},vap}$ are computed separately. This is similar to the approach used in the TRACE code for pressure gradient due to wall friction,

$$f_{\text{wall friction},liq} = -C_{wl} u_{liq} |u_{liq}| \tag{38}$$

and

$$f_{\text{wall friction},vap} = -C_{wg} u_{vap} |u_{vap}|\,. \tag{39}$$

A two-phase multiplier concept has been widely used in the prediction of two-phase flow

pressure drop due to wall friction. In the TRACE manual, based on such a two-phase multiplier concept, the wall friction coefficient is defined as,

$$C_{wl} = \Phi_l^2 \left[\frac{2 f_{2\Phi,l} (1-\alpha)^2 \rho_{liq}}{D_h} \right] \tag{40}$$

for the liquid phase wall friction coefficient. Here Φ_l^2 is the two-phase multiplier, and $f_{2\Phi,l}$ is the friction factor if the liquid phase flows alone in the channel. Note that the subscript l used here is an abbreviation for the *liquid* phase, equivalent to subscript *liq*. The wall friction coefficient for the vapor phase is defined similarly. In the bubbly flow regime, it is suggested to consider the effect of the presence of vapor bubbles on wall friction. In TRACE, for the bubbly flow regime, the wall friction coefficient for the liquid phase is calculated as,

$$C_{wl} = f_{wl} \frac{2\rho_l}{D_h} (1 + C_{NB})^2 \tag{41}$$

in which, f_{wl} is the single-phase liquid friction factor; and C_{NB} is a parameter considering the effect of bubble size and void fraction. In addition, TRACE manual also suggestes $C_{wg} = 0$ for all pre-CHF flow regimes.

In the two-phase *SEM*, the volumetric heat transfer between each phase and the interface are modeled as $A_{int} h_{conv,liq} (T_{int} - T_{liq})$ and $A_{int} h_{conv,vap} (T_{int} - T_{vap})$ for the liquid-to-interface and the vapor-to-interface heat transfer, respectively. The interface temperature, T_{int}, is the saturation temperature corresponding to the interface pressure, p_{int}. In TRACE and other existing system analysis codes using single-pressure two-phase model, the interface temperature is defined as the saturation temperature corresponding to the local pressure. This is noted as one of the major differences between the fully nonequilibrium, two-pressure, two-phase *SEM* and the traditional single-pressure two-phase flow models. In RELAP-7 all of the phase interactions terms include the interfacial area density A_{int} because they represent transfer terms that must pass mass, force, or energy through the interface. Simlarly, in TRACE, this interfacial area density and phasic interfacial heat transfer coefficient are both flow regime dependent. For bubbly flow, the interfacial area density is related to bubble size and void fraction,

$$A_{int} = \frac{6\alpha_{DB}}{d_{DB}} \frac{1-\alpha}{1-\alpha_{DB}} \tag{42}$$

and the liquid-to-interface heat transfer coefficient is calculated as,

$$h_{conv,liq} = \frac{k_{liq}}{d_{DB}} Nu_{DB} \tag{43}$$

where the Nusselt number is given by,

$$Nu_{DB} = 2.0 + 0.6 Re_{DB}^{1/2} Pr_{liq}^{1/3} . \tag{44}$$

Subscript 'DB' denotes dispersed bubble. d_{DB} is the diameter of dispersed bubble. α_{DB} is the transitional void fraction between bubbly flow and slug flow regimes. For the vapor-to-interface heat transfer coefficient in bubbly flow, a constant number is used,

$$h_{conv,vap} = 1000(W/m^2K) \tag{45}$$

Wall heat transfer coefficients in the pre-CHF regimes are normally flow regime independent. However, instead of directly providing a two-phase flow heat transfer coefficient, heat flux correlations are provided. For nucleate boiling, the TRACE manual suggests to use,

$$q''_{NB} = \left[(q''_{FC})^3 + (q''_{PB} - q''_{BI})^3 \right]^{1/3} \tag{46}$$

in which, q''_{FC} is forced convection heat flux. q''_{PB} is pool boiling heat flux. q''_{BI} is the fully developed boiling heat flux at the point of boiling initiation. When subcooled flow boiling takes place, additional correlations are needed for the heat flux partitioning between phase change and liquid phase sensible heat.

Table 1 summarizes the current status of implementation of flow regime related closure correlations, with ■ representing implemented and □ representing on-going/future task. Additional work is needed to link these closure correlations with equations, i.e., MOOSE kernels in the RELAP-7 code. Similarly, Figure 3 and Figure 4 show pre-CHF flow regimes in horizontal pipes and post-CHF flow regimes in vertical pipes, respectively. Table 2 and Table 3 summarize the current status of code implementations for these two regions. As it can be noticed, these are planned for future work.

In addition to these aforementioned flow regime related closure correlations, models to determine critical heat flux (CHF) will also be included in future work. Parallel to the

Table 1. Closure correlations related to pre-CHF flow regimes in vertical pipes

	Bubbly	Cap/slug	Annular mist
Wall drag	■	■	■
Interfacial drag	■	■	□
Interfacial heat/mass transfer	■	■	□
Wall heat transfer	■	■	■

implementation and improvement of closure correlations, corroborative support and validation work will also be performed on the RELAP-7 system code (two-phase models, equations of state, closure correlations, and coding) via simulations of nuclear reactor systems, components, and special effects tests. The validation work will follow the guidelines proposed in RELAP-7 validation plan [11].

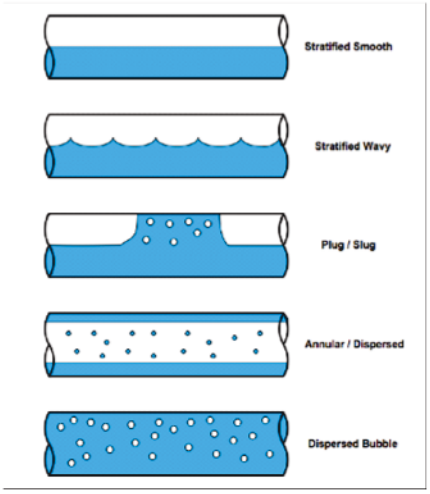

Figure 3. Flow regimes in horizontal pipes used in TRACE code [10]

Table 2. Closure correlations related to pre-CHF flow regimes in horizontal pipes

	Stratified smooth	Stratified wavy/Plug-slug	Annular/ dispersed	Dispersed bubbly
Wall drag	☐	☐	☐	☐
Interfacial drag	☐	☐	☐	☐
Interfacial heat/mass transfer	☐	☐	☐	☐
Wall heat transfer	☐	☐	☐	☐

Table 3. Closure correlations related to post-CHF flow regimes in vertical pipes

	Inverted annular	Inverted slug	Dispersed flow
Wall drag	☐	☐	☐
Interfacial drag	☐	☐	☐
Interfacial heat/mass transfer	☐	☐	☐
Wall heat transfer	☐	☐	☐

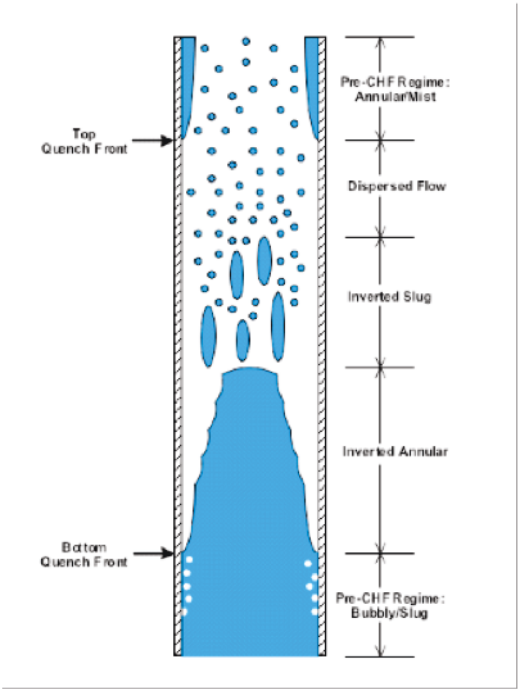

Figure 4. Post-CHF flow regimes in vertical pipes used in TRACE code [10]

References

[1] R. A. Berry, J. W. Peterson, H. Zhang, R. C. Martineau, H. Zhao, L. Zou, and D. Andrs, "RELAP-7 theory manual," Tech. Rep. INL/EXT-14-31366 (Rev. 1), Idaho National Laboratory, U.S.A., 2014.

[2] M. Kunick and H.-J. Kretzschmar, "Guideline on the fast calculation of steam and water properties with the spline-based table look-up method (SBTL)," tech. rep., The International Association for the Properties of Water and Steam, Moscow, Russia, 2015.

[3] M. Kunick, "Fast calculation of thermophysical properties in extensive process simulations with the spline-based table look-up method (SBTL)," tech. rep., VDI Fortschritt-Berichte, Germany, 2015. in preparation.

[4] M. Kunick, H.-J. Kretzschmar, F. di Mare, and U. Gampe, "CFD analysis of steam turbines with the iapws standard on the spline-based table look-up method (SBTL) for the fast calculation of real fluid properties," in *Proc. ASME Turbo Expo 2015: Turbine Tech. Conf. and Exposition*, (U.S.A.), American Society of Mechanical Engineers, 2015. Montreal, Canada.

[5] H. Spath, *Two Dimensional Spline Interpolation Algorithms*. Wellesly, MA, U.S.A.: A. K. Peters, 1995.

[6] M. O. Delchini, J. C. Ragusa, and R. A. Berry, "Entropy-based viscous regularization for multi-dimensional euler equations in low-mach and transonic flows," *Computers & Fluids*, vol. 118, pp. 225–244, 2015.

[7] R. M. Bowen, *Introduction to Continuum Mechanics for Engineers*. New York, U.S.A.: Plenum Press, 1989.

[8] M. O. Delchini, J. C. Ragusa, and R. A. Berry, "Viscous regularization for the non-equilibrium seven-equation two-phase flow model," 2015. submitted for publication, in review.

[9] R. C. Martineau, H. Zhang, and H. Zhao, "RELAP-7 beta release: Summary of capabilities," Tech. Rep. INL/EXT-14-33991, Idaho National Laboratory, U.S.A., 2014.

[10] "TRACE V5.0 theory manual: Field equations, solution methods, and physical models," tech. rep., U. S. Nuclear Regulatory Commission, U.S.A., 2007.

[11] C. L. Smith, Y. J. Choi, and L. Zou, "RELAP-7 software verification and validation plan," Tech. Rep. INL/EXT-14-33201, Idaho National Laboratory, U.S.A., 2014.


INL
Idaho National Laboratory